Deterministic Quantum Mechanics: Classical nuclear motion explains chemical reactions and spectra

Erik Rohloff, Dominik A. Rudolph, Onno Strolka, and Irmgard Frank*

Universität Hannover, Theoretische Chemie, Callinstr. 3A, 30167 Hannover, Germany

October 6, 2021

Abstract

Is a classical description of nuclear motion sufficient when describing chemical reactions? The present paper investigates some phenomena that were previously attributed to nuclear quantum effects. The aim is to show that these phenomena can be modelled with traditional Car-Parrinello molecular dynamics, that is, with a method which treats nuclear motion classically. We find that no additional paradigm is needed for describing chemical reactions. The special reactivity observed for carbenes can be attributed to the special environment represented by a noble gas matrix. Also the infrared spectrum of porphycene is perfectly modelled by traditional Car-Parrinello molecular dynamics. If no more convincing examples are produced, one will stick to deterministic quantum mechanics, as it is the simpler theory which, in addition, is free of paradoxa.

Keywords

Deterministic quantum mechanics, Car-Parrinello molecular dynamics, reaction mechanisms

1

1 Introduction

Quantum chemistry is the application of the Schrödinger equation to matter of any kind. Generally, matter consists in an electronic wavefunction and in an accumulation of nuclei. Soon after the publication by Schrödinger it became clear, that, to make the problem tractable, one should compute electronic structure and nuclear motion separately. To this end the Born-Oppenheimer approximation was formulated. Within this approximation, the total wavefunction is described as a product of electronic and nuclear wavefunctions. Then, the electronic and nuclear problem are separated. Unfortunately, the interaction between electronic and nuclear system is non-negligible. Even worse, it turns out, that the nuclear-nuclear interaction must be added to the electronic energy if one wants to obtain what is called Born-Oppenheimer surfaces or also potential energy surfaces, PES. Hence, the only term which is not described in normal quantum chemical calculations, is the kinetic energy of the nuclei. That is, in normal quantum chemical calculations, we describe the situation at zero Kelvin. What is left for the nuclei? Car and Parrinello gave the answer with their extended Lagrangian [1]. They describe the electronic cloud with the density functional approximation and the nuclear motion with classical Newton theory. This results directly from a consistent description of the nuclei as classical point charges. Car and Parrinello also proposed to introduce a quasi-classical treatment of the electrons. 'Quasi-classical' is an understatement, as the equations look much the way they should in a quantum-field theory: We have second derivatives with respect to time and space. In the present work we are not concerned with the question how good this treatment of the electrons is: The considerations concerning nuclear motion are independent on the description of electronic motion with Car-Parrinello molecular dynamics or, alternatively, Born-Oppenheimer molecular dynamics,

where the system is quenched to the Born-Oppenheimer surface in every step.

Based on our experience with the simulation of chemical reactions, and particularly of photoreactions [2, 3, 4, 5], we claim that using Newton dynamics instead of the Schrödinger equation for the nuclei is not just a cheap approximation. We gain nothing by describing the nuclear motion quantum mechanically. On the contrary: A quantum mechanical description of nuclear motion leads to all kinds of paradoxa. We got used to believing in these paradoxa, but it is a relieve to discard them. This is possible with the very simple idea that electronic structure and nuclear motion are best described using different approaches: quantum mechanics and Newton dynamics, respectively. In this picture, all tunneling effects observed are due to electronic tunneling. Experimentally observed isotope effects can have different origins. For every quantity traditionally explained with quantum effects it must be asked, if these effects are also obtained when using Newton dynamics. Mass certainly plays a role in Newton dynamics, F = m * a. Hence we do describe kinetic isotope effects correctly. Typically our simulations are slower if heavier isotopes are used. To decide about static isotope effects, all the different phenomena described as isotope effects must be investigated. For example, we do not get isotope effects which are due to vibrational zero point energy, since our classical nuclei have no vibrational zero point energy. In contrast, temperature effects like bond-length elongation are correctly obtained with a classical description of nuclear motion.

Recently, two examples have been published with the intention to prove quantum mechanical nuclear motion: The isomerization of carbenes [6, 7] and the infrared spectrum of porphycene [8, 9]. In the present paper we investigate these phenomena using the classical

part of the Car-Parrinello molecular dynamics code.

2 Results and Discussion

2.1 Isomerization of methylhydroxycarbene

Schreiner et al. [6, 7] investigated a highly interesting reaction, namely the isomerization of carbenes, in particular the isomerization of methylhydroxycarbene **1**. This compound can in principle undergo the thermal isomerization to acetaldehyde **2** via transition state TS1 or to vinyl alcohol **3** via transition state TS2 (see Figure 1). Experimentally, at low temperatures the more stable product **2** is observed, even if the reaction barrier is higher than that for the reaction to product **3**.
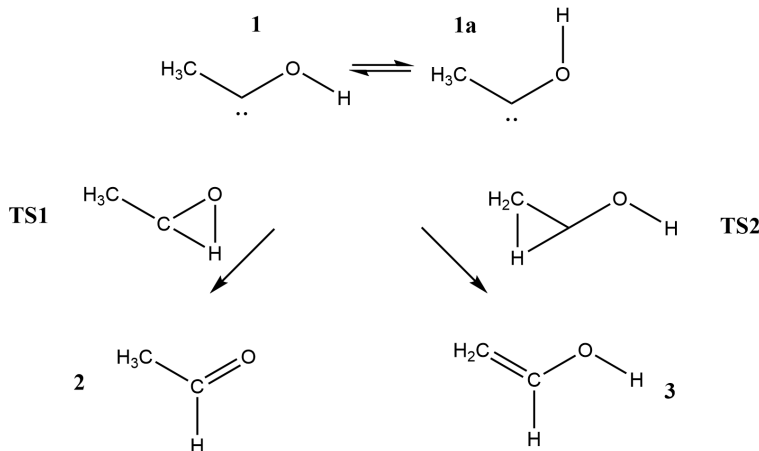

Figure 1: Reactions starting from methylhydroxycarbene **1** as discussed in Refs. [6] and [7]. Experimentally, acetaldehyde **2** is formed.

On this basis Schreiner introduced a third reactivity paradigm, besides thermodynamic or kinetic control. He attributed the observation of **2** to nuclear tunneling through the narrower barrier. This explanation is unpleasant since the width of a barrier is not well-defined in contrast to the height of a barrier. The latter one

has the unit of an energy and corresponds to a difference of state functions. In contrast, the width of a barrier may be a combination of parameters like bond distances, angles, etc. In three-dimensional space, it is not well-defined.

If an expected product is not observed, this may have several reasons, including an alternative decomposition. In such a situation, Car-Parrinello molecular dynamics may be helpful. What do we find, if we investigate the reactions of methylhydroxycarbene using Car-Parrinello molecular dynamics simulations? First, it has to be emphasized that we cannot simulate the full reaction, this would take quadrillions of CPU hours. We must accelerate the reactions in some way. As we do not want to restrict the reaction pathway to certain degrees of freedom, we can get an acceleration only by raising the temperature. Of course this is not the same as simulating the full reaction at low temperatures, but we can get some information about possible reaction pathways that might have been overlooked. The result is summarized in Table 1. We did simulations ranging from 2000 to 10000 K. Only the simulations for 6000 K and above are listed. At lower temperatures no reactions were observed on the picosecond timescale, with the exception of a single simulation run where a reaction to **3** was observed already at 4000 K.
We performed simulations for the two isomers of methylhydroxy-carbene, **1** and **1a**. **1** and **1a** reacted in a similar way. At high temperatures, the reaction to both compounds **2** and **3** is observed. Several aspects are striking: **3** can be converted into the thermodynamic product **2** via a four-membered-ring transition state **TS3**, see Figures 2 and 3. In a single case also the back reaction is observed. Furthermore, increasing the argon pressure leads to a more efficient formation of **2**. Finally, decomposition to products like CO, H_2 and H_2O is observed. In the gas phase, the decomposition is predomi-
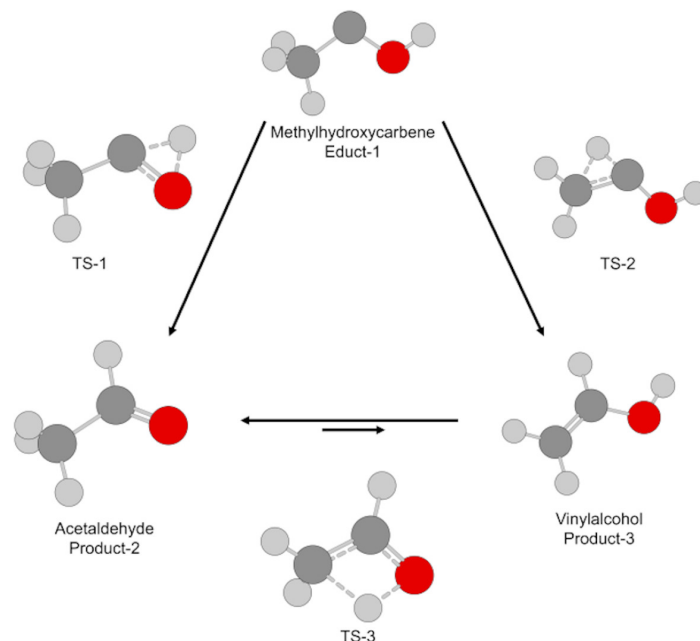
nant.

Figure 2: Sketch of the reactions starting from methylhydroxycarbene **1**. In addition to transition states **TS1** and **TS2** there is yet another transition state **TS3** which explains the experimental observations.

The latter observation is due to the exothermicity of the reactions. A high amount of potential energy is converted into kinetic energy which leads to decomposition. This is different if the molecules are environed by an argon matrix. The matrix forms kind of a nanoreactor as it was introduced by Martinez [10]. By using the CPMD code, we are employing a different concept to realizing such a nanoreactor, namely periodic boundary conditions and an explicit solvent or environment. The effect is the same: The reactive species is contained in a small space, the atoms can hardly escape on the
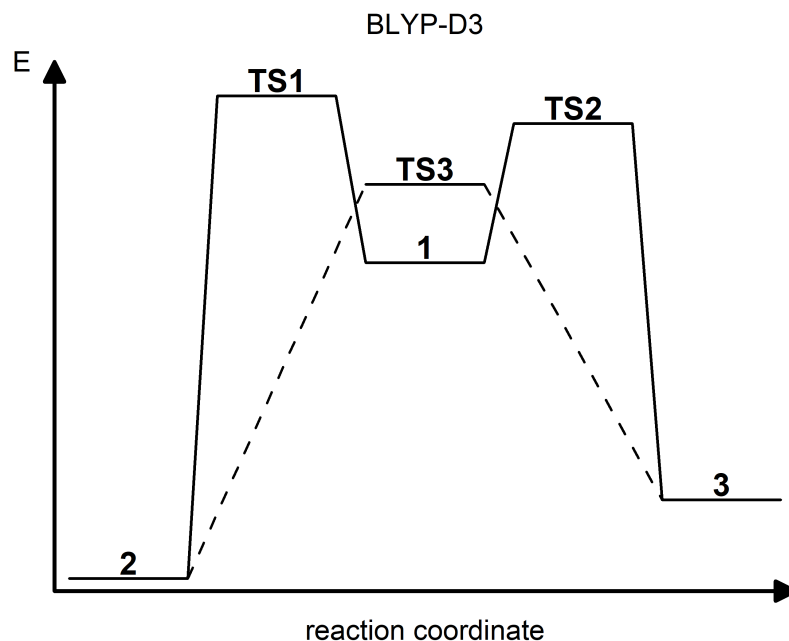
Figure 3: Sketch of the energetics of the reactions starting from methylhydroxycarbene **1**. Via transition state **TS3** the thermodynamic product **2** can be formed.

timescale of the reaction. At the same time, kinetic energy is transfered to the environment, respectively the matrix, thus preventing thermal decomposition.

Finally, the transition state **TS3** explains why only the thermodynamic product is observed in experiment. In our simulations, an equal amount of **2** and **3** is formed in the end whereby the normal route is **1** / **1a** → **3** → **2**. Already on the picosecond time scale this reaction pathway shifts the result strongly in the direction of **2**. On experimental time scales this will lead nearly exclusively to the formation of **2** in an amount determined by the energy difference between **2** and **3**, that is, the thermodynamical product will be

obtained predominantly.

Isomer	Argon atoms	Temperature [K]	Intermediate	Time [ps]	Final product	Time [ps]
1	0	6000	-	-	-	-
1	0	8000	**3**	0.71	H_2O	0.84
1	0	10000	**2**	0.09	CO	0.10
1	24	6000	-	-	**3**	0.39
1	24	8000	-	-	CO	0.35
1	24	10000	**2**	0.22	H_2	0.34
1	32	6000	-	-	**2**	0.44
1	32	8000	**3**	0.17	**2**	0.67
1	32	10000	**3**	0.19	H_2	0.22
1	40	6000	**3**	0.20	**2**	0.59
1	40	8000	**3**	0.02	**2**	2.37
1	40	10000	-	-	H_2	0.77
1a	0	6000	-	-	CO	0.34
1a	0	8000	-	-	CO	0.33
1a	0	10000	-	-	CO	0.31
1a	24	6000	**3**	0.26	H_2	0.56
1a	24	8000	-	-	**3**	0.06
1a	24	10000	**3**	0.01	H_2O	0.40
1a	32	6000	-	-	H_2	0.43
1a	32	8000	-	-	**3**	0.03
1a	32	10000	**3**	0.02	H_2	0.14
1a	40	6000	H_2O	0.17	**3**	0.65
1a	40	8000	-	-	**3**	0.20
1a	40	10000	**3**	0.05	**2**	0.28

Table 1: Protocol of the CPMD simulations. The total simulation time of every run was 2.66 ps. The most relevant products are specified. The most important product is compound **2**. Compound **3** is often converted to **2**. Also the back reaction is observed. Cleavage of H_2O, CO or H_2 means complete decay. Not listed are the simulations at lower temperatures than 6000 K because only one of them led to a reaction.

Compound	BLYP	B3LYP	BLYP-D3	B3LYP-D3	HF	MP2	B2PLYP	B2PLYP-D3
1	52.1	51.6	52.4	52.0	47.6	54.9	52.6	52.7
2	0.0	0.0	0.0	0.0	0.0	0.0	0.0	0.0
3	12.9	12.5	13.1	12.8	14.6	14.6	13.7	13.8
TS1	79.8	83.7	80.1	84.0	97.2	84.4	83.8	84.0
TS2	75.3	76.6	75.5	76.8	83.3	80.1	78.2	78.3
TS3	65.3	69.5	65.5	69.7	86.9	71.0	70.6	70.6

Table 2: Energetics (in kcal/mol) as computed with Gaussian. All methods agree well. The largest deviations are obtained with Hartree-Fock.

2.2 Infrared spectrum of porphycene

Rossi and coworkers [8] investigated the infrared spectrum of porphycene (Figure 4).
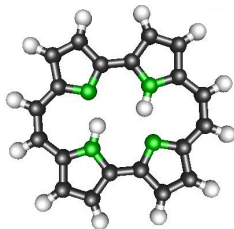
Figure 4: Porphycene.

They attributed a feature at about 2500 cm^{-1} to a quantum mechanical nuclear motion. We did several calculations to elucidate this phenomenon. We started from static calculations performed with the Gaussian program package (Figures 5 and 6). The first observation is, that there is certainly no agreement within 50 cm^{-1}, the error of the electronic structure methods is larger. The dispersion correction has only a minor influence. The experimental absorption around 2500 cm^{-1} is missing completely in the calculations. All methods agree in this point.

This changes, if temperature is applied in a Car-Parrinello molecular dynamics simulation (Figures 7 and 8). Figure 7 displays the results without dispersion correction, Figure 8 is with dispersion correction. At 10 Kelvin there is only weak absorption in the region between 2000 and 3000 K. This changes strongly, if the temperature is raised. In the simulation at 290 K without dispersion correction we get a pattern which agrees best with the experiment (see Figure 4d in Ref. [11]) . We observe, that the agreement of electronic structure methods with experiment is a bit accidental, while the application of temperature is necessary.
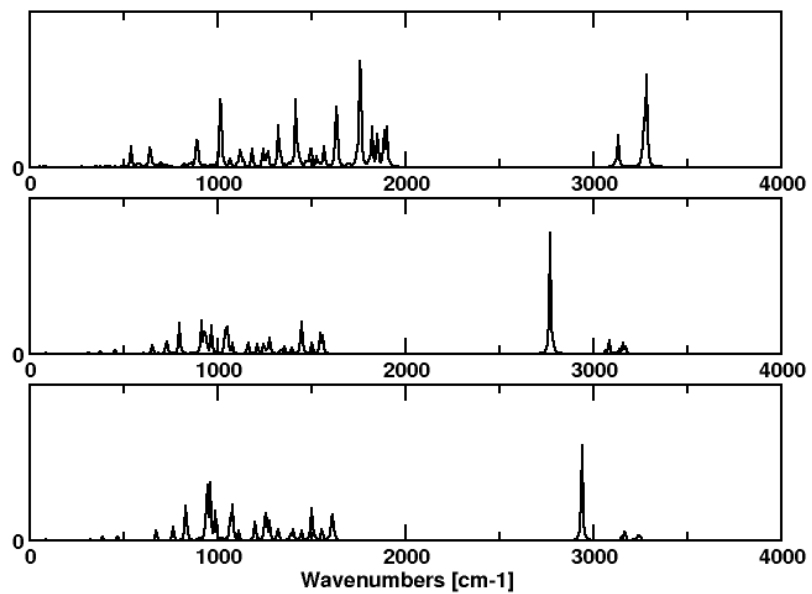
Figure 5: Infrared spectra of porphycene computed with Gaussian (at zero Kelvin). From top to bottom: AM1, BLYP, B3LYP.
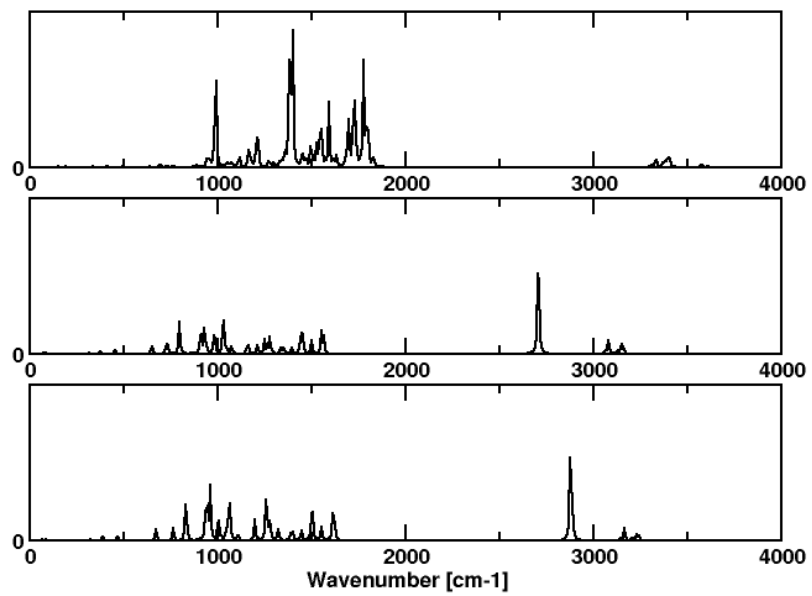
Figure 6: Infrared spectra of porphycene computed with Gaussian (at zero Kelvin). From top to bottom: HF, BLYP-D, B3LYP-D.
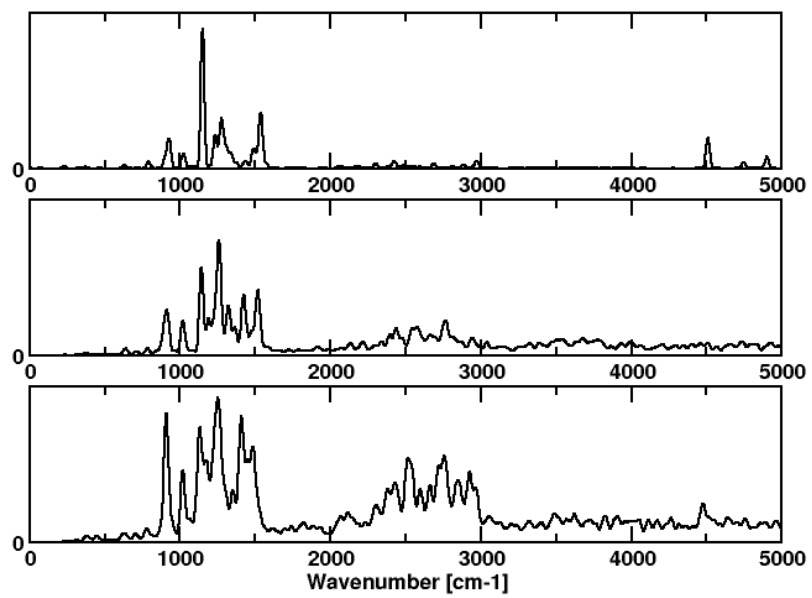
Figure 7: Infrared spectra of porphycene computed with CPMD/BLYP and TRAVIS. From top to bottom: 10 K, 290 K, 550 K. The spectrum at 290 K fits best to experiment.
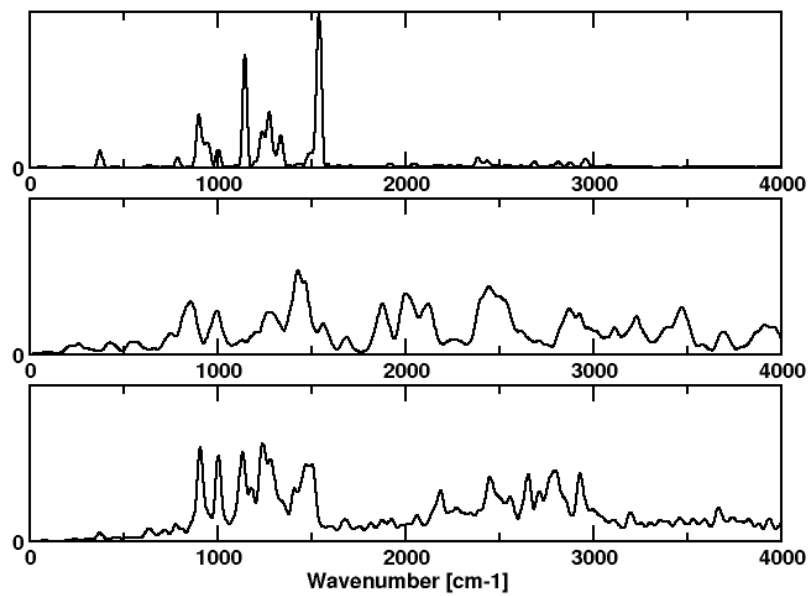
Figure 8: Infrared spectra of porphycene computed with CPMD/BLYP-D and TRAVIS. From top to bottom: 10 K, 280 K, 550 K.

3   Conclusions

We have simulated phenomena that were recently reported with the intention to prove quantum mechanical nuclear motion. We find alternative explanations for the observations.

The reaction of methylhydroxycarbene **1** to acetaldehyde **2** is readily explained by an additional transition state for the reaction route **1** → **3** → **2**. The thermodynamical product is efficiently formed. Also the back reaction is possible. In the end a distribution according to the energy difference of the products will be obtained. As a result, **2** is the dominating product. An important parameter is the argon matrix. The higher the argon pressure, the more likely the formation of **2**. Without a surrounding matrix, the decomposition to a variety of products is dominant. Hereby, the matrix has two effects, namely keeping the atoms together and taking up the energy which is set free in these exothermic reactions. To conclude, the CPMD simulations show the reaction to the experimentally observed thermodynamical product. An additional paradigm is not needed.

The picture is the same for the infrared spectrum of porphycene. It is obvious that for medium-sized molecules the computation of accurate infrared spectra is problematic. This is primarily due to the lack of thermal motion in static quantum chemical calculations and to the lack of accuracy of the electronic structure methods. It is obvious that application of temperature, as it is possible in a molecular dynamics simulation, represents a clear improvement. The application of path-integral calculations has a similar effect. One might argue that temperature is certainly present in experiment while we are not sure about nuclear quantum effects. Also in this case it is possible to explain the experimental observations

without advocating nuclear quantum effects. It should be emphasized that temperature can play a major role for computing infrared spectra and can hardly be omitted.

To conclude, a clear deviation from experiment caused by the neglect of nuclear quantum effects is missing. All studies, which claim the opposite, report effects that are in the range of the error of electronic structure methods. A clear difference like an ultraviolet catastrophe is missing [12]. We get no hint from experiment how to improve our classical scheme. There is no reason to introduce quantum nuclear motion to explain molecular structure and chemical reactions. In contrast, the quantum mechanical description of the electronic structure is essential and explains all the fascinating richness of molecular structure, five-membered and six-membered rings, catenanes, ladderenes, fullerenes, nanotubes, Feringa's nanorotor, DNA, and many more. Finally, electronic tunneling is most important when describing chemical reactions.

4 Methods

Car-Parrinello molecular dynamics simulations [1, 13, 14] have been performed in the NVE ensemble using the Becke-Lee-Yang-Parr (BLYP) functional in connection with the Grimme dispersion correction [15]. In the case of the carbene isomerization, the time step was chosen as 1 a.u. (0.024 fs) and the fictitious electron mass as 100 a.u. This relatively small time step is needed for describing the high-temperature scenario accurately. Troullier-Martins pseudopotentials as optimized for the BLYP functional were employed for describing the core electrons [16, 17]. For the reactive simulations, the spin-unrestricted version of Kohn-Sham theory was employed [18]. The plane-wave cutoff which determines the size of the basis

set, was set to 70.0 Rydberg. The simulation cell size was 16 x 16 x 16 $a.u.^3$ (8.5 x 8.5 x 8.5 $\mathring{A}^3$). Argon matrices with different densities were created: gas phase (0 argon atoms), low pressure (24 argon atoms), normal pressure (32 argon atoms), high pressure (40 argon atoms). After equilibration of stable, neutral closed-shell systems, the initial temperature was set to 2000, 4000, 6000, 8000, and 10000 K. During the production runs, the temperature was not controlled. A list with the different simulation protocols is contained in Table 1.

For comparison, Gaussian calculations [19] were performed using BLYP, B3LYP, BLYP-D3, B3LYP-D3, Hartree-Fock, MP2, B2PLYP and B2PLYP-D3 [19, 20, 21, 15, 22]. The basis set was chosen to be 6-311G(d,p).

In the case of porphycene, a time step of 5 a.u. (0.12 fs) and a fictitious electron mass of 400 a.u. was chosen which was sufficient to get stable simulations. The plane-wave cutoff was set to 50.0 Rydberg, as the system contains no problematic atoms. The simulation cell size was 24 x 24 x 24 $a.u.^3$ (12.7 x 12.7 x 12.7 $\mathring{A}^3$) to allow for free rotation. Porphycene was optimized, then the TEMPERATURE IONS option was used to set the start energy to 6, 600 and 1200 K respectively. As more or less half of the energy is converted into potential energy, this resulted in temperatures of about 10, 290, and 550 K. During the production runs, the temperature was not controlled. Wannier centers were computed using the DIPOLE DYNAMICS keyword. The TRAVIS program [23] was used to compute the spectra from the trajectories.

For comparison, frequency calculations with the Gaussian program package [19] were performed using AM1, Hartree-Fock, BLYP, B3LYP, BLYP-D, and B3LYP-D [19, 24, 20, 21, 25]. The basis set was chosen to be 6-311G(d,p).

5 Funding Information

6 Research Resources

References

[1] R. Car, M. Parrinello, *Phys. Rev. Lett.* **1985**, *55*, 2471–2474.

[2] U. Röhrig, L. Guidoni, A. Laio, I. Frank, U. Röthlisberger, *J. Am. Chem. Soc.* **2004**, *126*, 15328.

[3] S. Grimm, C. Bräuchle, I. Frank, *Chem. Phys. Chem.* **2005**, *6*, 1943.

[4] I. Frank, K. Damianos, *J. Chem. Phys.* **2007**, *126*, 125105.

[5] J. Friedrichs, I. Frank, *Chem. Eur. J.* **2009**, *15*, 10825.

[6] P. R. Schreiner, H. P. Reisenauer, D. Ley, D. Gerbig, C.-H. Wu, W. D. Allen, *Science* **2011**, *332*, 1300.

[7] P. R. Schreiner, *J. Am. Chem. Soc.* **2017**, *139*, 15276–15283.

[8] Y. Litman, J. O. Richardson, T. Kumagai, M. Rossi, *J. Am. Chem. Soc.* **2019**, *141*, 2526.

[9] S. Gawinkowski, L. Walewski, A. Vdovin, A. Slenczka, S. Rols, M. R. Johnson, B. Lesyng, J. Waluk, *Phys. Chem. Chem. Phys.* **2012**, *14*, 5489.

[10] L.-P. Wang, A. Titov, R. McGibbon, F. Liu, V. S. Pande, T. J. Martinez, *Nature Chem.* **2014**, *6*, 1044.

[11] Y. Litman, D. Donadio, M. Ceriotti, M. Rossi, *J. Chem. Phys.* **2018**, *148*, 102320.

[12] R. C. Büchel, D. A. Rudolph, I. Frank, *Int. J. Quantum Chem.* **2021**, *121*, e26555.

[13] D. Marx, J. Hutter, *Ab Initio Molecular Dynamics: Basic Theory and Advanced Methods*, Cambridge University Press, Cambridge, **2009**.

[14] Version 4.1, J. Hutter et al., http://www.cpmd.org/, Copyright IBM Corp 1990-2015, Copyright MPI für Festkörperforschung Stuttgart 1997-2001.

[15] S. Grimme, *J. Comput. Chem.* **2006**, *27*, 1787–1799.

[16] N. Troullier, J. L. Martins, *Phys. Rev. B* **1991**, *43*, 1993.

[17] M. Boero, M. Parrinello, K. Terakura, H. Weiss, *Mol. Phys.* **2002**, *100*, 2935–2940.

[18] O. Gunnarsson, B. I. Lundqvist, *Phys. Rev. B* **1976**, *13*, 4274.

[19] M. J. Frisch, G. W. Trucks, H. B. Schlegel, G. E. Scuseria, M. A. Robb, J. R. Cheeseman, G. Scalmani, V. Barone, G. A. Petersson, H. Nakatsuji, X. Li, M. Caricato, A. V. Marenich, J. Bloino, B. G. Janesko, R. Gomperts, B. Mennucci, H. P. Hratchian, J. V. Ortiz, A. F. Izmaylov, J. L. Sonnenberg, D. Williams-Young, F. Ding, F. Lipparini, F. Egidi, J. Goings, B. Peng, A. Petrone, T. Henderson, D. Ranasinghe, V. G. Zakrzewski, J. Gao, N. Rega, G. Zheng, W. Liang, M. Hada, M. Ehara, K. Toyota, R. Fukuda, J. Hasegawa, M. Ishida, T. Nakajima, Y. Honda, O. Kitao, H. Nakai, T. Vreven, K. Throssell, J. A. Montgomery, Jr., J. E. Peralta, F. Ogliaro,

M. J. Bearpark, J. J. Heyd, E. N. Brothers, K. N. Kudin, V. N. Staroverov, T. A. Keith, R. Kobayashi, J. Normand, K. Raghavachari, A. P. Rendell, J. C. Burant, S. S. Iyengar, J. Tomasi, M. Cossi, J. M. Millam, M. Klene, C. Adamo, R. Cammi, J. W. Ochterski, R. L. Martin, K. Morokuma, O. Farkas, J. B. Foresman, D. J. Fox, *Gaussian˜16 Revision A.03*, **2016**, Gaussian Inc. Wallingford CT.

[20] A. Becke, *Phys. Rev. A* **1988**, *38*, 3098–3100.

[21] A. Becke, *J. Chem. Phys.* **1993**, *98*, 1372–1377.

[22] S. Grimme, *J. Chem. Phys.* **2006**, *124*, 034108.

[23] M. Thomas, M. Brehm, R. Fligg, P. Vöhringer, B. Kirchner, *Phys. Chem. Chem. Phys.* **2013**, *15*, 6608.

[24] M. J. S. Dewar, E. G. Zoebisch, E. F. Healy, J. J. P. Stewart, *J. Am. Chem. Soc.* **1985**, *107*, 3902.

[25] S. Grimme, *J. Comput. Chem.* **2004**, *25*, 1463.